TECHNICAL PAPER

Multidirectional vortices mixing in three-stream micromixers with two inlets

Rei-Tang Tsai · Chih-Yang Wu

Abstract In this work, we design, fabricate and compare three types of three-stream curved-straight-curved (CSC) micromixers, including the full three-stream (FTS) CSC micromixer, the CSC microchannel with internal side-wall injection and the CSC microchannel with external side-wall injection. In the three-stream CSC micromixers, there is a core stream sandwiched by two cladding streams into the CSC channel with baffles from two inlets. The sandwiched structure of streams and the multidirectional vortices due to flow separation and channel curvature contribute together to enhance mixing. We examine fluid mixing in the proposed micromixers by numerical simulation and using confocal spectral microscope imaging system. The present results show that the mixing efficiency increases without increasing the pressure applied much by the channel structure forming the sandwiched structure of streams. Besides, it is found that the FTS CSC micromixer is the preferable one among the micromixers considered.

1 Introduction

Micromixer is a key component of the lab-on-a-chip (LOC). This is because many biochemical processes, such as enzyme reactions, protein folding and cell activation, require rapid and uniform mixing (Tay 2002). Because of the small lateral size of the microchannel, the flow is predominantly laminar. Hence, rapid mixing of fluids in the microfluidic system is difficult to achieve and remains a challenge.

R.-T. Tsai · C.-Y. Wu (✉)
Department of Mechanical Engineering,
National Cheng Kung University, Tainan 70101, Taiwan, ROC
e-mail: cywu@mail.ncku.edu.tw

In recent years many ingenious micromixers have been designed and developed (Hessel et al. 2005; Nguyen and Wu 2005), and those can be classified into two types, active micromixers and passive micromixers. Active micromixers utilize external forces and/or moving parts to disturb the flow of mixing fluids. Passive micromixers enhance mixing with the features of microchannel geometries, which increase the interfacial area of different fluids or decrease the diffusion length. In general, active micromixers have a better mixing efficiency than passive micromixers. However the designs of active micromixers are often difficult to integrate with other microfluidic components and add substantial complexity to the fabrication processes. By contrast, it is simpler to fabricate passive micromixers and easy to integrate them with microfluidic systems. Therefore, passive micromixers still gain attention and have been developed widely.

Various geometry structures have been proposed to enhance mixing in passive micromixers. Comparison of micromixers based on chaotic advection in three-dimensional (3D) structures and those designs based on planar structures shows that the 3D structures are better at mixing, but their fabrication requires either multi-step lithography or aligned assembly of multiple layers (Chen and Meiners 2004; Liu et al. 2000; Stroock et al. 2002). In planar micromixers, effective mixing can be obtained by lamination (Abonnenc et al. 2009; Hessel et al. 2003; Wu and Nguyen 2005), hydrodynamic focusing (Knight et al. 1998), flow impinging (Bothe et al. 2006), Dean vortices (Jiang et al. 2004; Yi and Bau 2003), separation vortices (Bhagat et al. 2007; Chung et al. 2008; Wang et al. 2002) or a combination of the above strategies (Lee et al. 2010; Sudarsan and Ugaz 2006; Tsai and Wu 2011).

In this work, both numerical simulation and experiment are performed to investigate the effects of the number and

the location of fluid stream interfaces on mixing in the curved-straight-curved (CSC) channel with radial baffles shown in Fig. 1a. The geometry of the CSC channel with radial baffles produces multidirectional vortices which enhance fluid mixing (Tsai and Wu 2011). The solid lines in Fig. 1a describe a full three-stream (FTS) design, which allows three streams of liquids—a core stream sandwiched by two cladding streams—to flow into the CSC channel from two inlets. We call the micromixer shown in Fig. 1b an FTS CSC micromixer. Furthermore, we consider two other designs with different locations of the side-wall injection to examine the influence of the location of fluid stream interfaces resulting from different side-wall injections. One is the CSC channel with an internal side-wall injection (ISI) connected to the middle of the internal cylindrical wall between two baffles in the first mixing unit, and the other is the CSC channel with an external side-wall injection (ESI) connected to the middle of the external cylindrical wall between two baffles in the first mixing unit. The two side-wall injection channels are shown by dash lines in Fig. 1a. The flows of the two designs consist of three streams after the second passage. Most of the previous works, on the mixing of two fluids with one core stream being sandwiched between two outer streams, considered mixing in flows with parabolic velocity profiles (Abonnenc et al. 2009; Knight et al. 1998; Wu and

Nguyen 2005). In this work, we examine the mixing behaviors of the complicated three-stream flow with multidirectional vortices in the CSC channel for a wide range of the Reynolds number ($0.03 \leq Re \leq 81$). Here, the Reynolds number is defined as $Re = \bar{u}\, d_h\, v^{-1}$, where $\bar{u}$, d_h and v denote the mean velocity of the downstream flow, the hydraulic diameter of the main channel and the kinematic viscosity of the fluid, respectively.

2 Micromixer design

The proposed FTS micromixer is shown in Fig. 1a. The design consists of two mixing units which have a rectangular cross section of $W_m = 200$ μm by $H = 120$ μm. Each of the mixing units is a semicircle channel with two radial baffles; the first baffle is attached to the internal cylindrical wall and the second is attached to the external cylindrical wall. The semicircle channel has a radius of center line $R_c = 225$ μm and is the main part in which mixing is enhanced. Besides, the thickness (t) and the width (w) of the radial baffle equal to 40 and 150 μm, respectively, the interval between two neighboring radial baffles is defined by $\theta_b = 60°$, and the two mixing units are connected by a straight channel with $L_c = 600$ μm. The fluids A and B are introduced at two inlets with rectangular cross section $W_i = 100$ μm by $H = 120$ μm. The inlet channel of fluid A is then split into two side inlets with equal width $W_s = 50$ μm. The inlet channel of fluid B with a length L_i of 500 μm and the two side inlets of fluid A with a length L_s of 150 μm are connected to the CSC channel, and so the core stream of fluid B is sandwiched by two cladding streams of fluid A. The sandwiched structure with two stream interfaces is generated to double the interfacial area, and so the enhancement of fluid mixing can be expected. The length of the entrance channel before the first baffle of the CSC channel is $L_e = 400$ μm and the straight channel connecting the end of the second mixing unit and the exit has a length $L_o = 2,000$ μm.
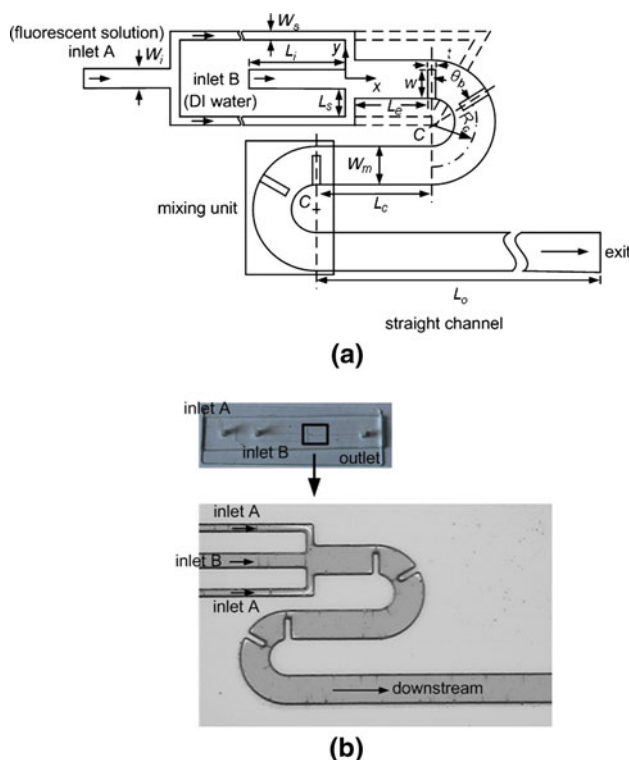
3 Numerical simulations

The mixing behavior of fluids in the micromixer is described by the continuity equation, the momentum equation and the species convection–diffusion equation for isothermal steady incompressible flow. The governing equations are solved by the computational fluid dynamics software (CFD-ACE). In this work, the SIMPLEC algorithm is used for pressure–velocity coupling, and the second order upwind scheme with limiter is adopted for the velocity and concentration calculations. The stopping criterion of iterative computation is that the relative residual

Fig. 1 a Schematic diagram of the FTS CSC micromixer and **b** overall view of the fabricated FTS CSC micromixer

for each variable is <0.0001. Furthermore, the no-slip condition is set on the solid walls and the pressure at the exit is set to be 1 atm.

We consider equal flow rate at both inlets, thus the mixing rate is 1:1. The mole fraction of fluorescent solution (Rhodamine B, Fluka, Germany) is set to be 1 at inlet A and 0 at inlet B, respectively. In this simulation, the physical properties of water are applied to the fluid in each of the inlets. The density, the viscosity and the diffusion coefficient of Rhodamine B in deionized (DI) water are 997 kg m^{-3}, 0.00097 kg m^{-1} s^{-1} and 3.6×10^{-10} m^2 s^{-1} (Rani et al. 2005), respectively. The velocity at each of the inlets is set to be a uniform profile corresponding to Reynolds numbers of 0.03, 0.1, 0.3, 1, 3, 9, 27, and 81. Those values of the Reynolds number are selected to cover the range of flows from the diffusion domination to the convection domination of the mixing.

To compare the mixing efficiency of micromixers with various flow conditions and geometrical parameters, the degree of mixing, M, (Boss 1986) is calculated by

$$M = 1 - \frac{\sigma}{\sigma_0} \tag{1}$$

where σ is the standard deviation of mole fraction at a transverse cross section defined by the expression

$$\sigma^2 = \frac{1}{n} \sum_{i=1}^{n} (c_i - \bar{c})^2 \tag{2}$$

with n denoting the total number of sampling, c_i the mole fraction at a position on the cross section considered and $\bar{c}$ the average value of c_i. At the beginning of the mixing process the two fluids are segregated and the standard deviation can be expressed by

$$\sigma_0^2 = \bar{c}(1 - \bar{c}) \tag{3}$$

Besides, $M = 0$ indicates the state before mixing, while $M = 1$ indicates complete mixing.

4 Fabrication and experimental setup

The channel pattern for the mixer is fabricated by planar micro-lithography processes. Initially, an 120 μm SU-8 (50) film (MicroChem, USA) is spun on the silicon wafer with a rotational speed of 650 rpm for 30 s. Then, the wafer with SU-8 film is heated for 15 min at 65 °C and 45 min at 95 °C. The wafer with SU-8 film is exposed to 365 nm UV light at 240 mJcm^{-2} to pattern the channel structure of micromixer. The wafer with SU-8 film is subsequently heated for 10 min at 65 °C and 15 min at 95 °C. After development process, the SU-8 master mold can be obtained. The polydimethylsiloxane (PDMS, Dow Corning Corp., USA) and curing agent at 8:1 ratio are mixed and poured onto the SU-8 mold. After curing at 100 °C for 60 min, the PDMS is peeled off from the mold. Then, both the PDMS and a sheet of glass are treated with oxygen plasma, brought into contact, and punched with each other to complete the bonding. Figure 1b shows an overall view of the fabricated FTS micromixer for further investigation.

The experimental apparatus for verifying the mixing behaviors in a pressure-driven flow includes two parts: the fluid flow system and the imagine processing system. During experiment, one syringe is filled with fluorescent solution, while the other is filled with DI water. The two syringes are driven at constant flow rates by a syringe pump (KDS 220, KD Scientific, USA) and are connected to the inlets of the micromixer shown in Fig. 1b. Confocal spectral microscope imaging system (TCS SP2, Leica Corp., Germany) is used to acquire the images for verifying the mixing behaviors of the two fluids in the micromixer. In this work, the images of concentration distributions on the horizontal cross section and those on the vertical cross section of the flow are obtained by scanning over the horizontal and the vertical cross sections, respectively, as shown in Fig. 2.

5 Results and discussion

The cells with varying sizes are used to reduce the effect of numerical diffusion. A preliminary cell size sensitivity study was performed to determine the sizes of cells used. The number of the cells in the tangential direction in each of the curved channels is set to be 270, and the numbers of cells in the x-direction in each of the straight channels with length, L_e, L_c, and, L_o equal to 80, 180, and 300, respectively. The numbers of cells in the y-direction for the straight channels and that in the radial direction in the part of curved channel without baffles are set to be 72. Besides, the number of the cells in the radial directional in the passages of the curved channel is set to be 48, and that in the vertical direction (normal to x- and y-axes) is set to be 24. Figure 2 shows that the simulated concentration distributions obtained by using the aforementioned cells are in reasonable agreement with those obtained by experiment at $Re = 1$, 9, and 81.

Figures 3 and 4 show the flow patterns, the concentration distributions and the velocity contours of the original CSC micromixer and the FTS CSC micromixer for the cases with $Re = 0.3$ and $Re = 27$, respectively. The mixing in the case with $Re = 0.3$ is dominated by diffusion, while the lateral advection is caused by converging–diverging flow and centrifugal force plays an important role in the fluid mixing for the case with $Re = 27$. From Figs. 3 and 4, one may find that the geometric sandwiched structure of fluid streams can increase the interfacial area
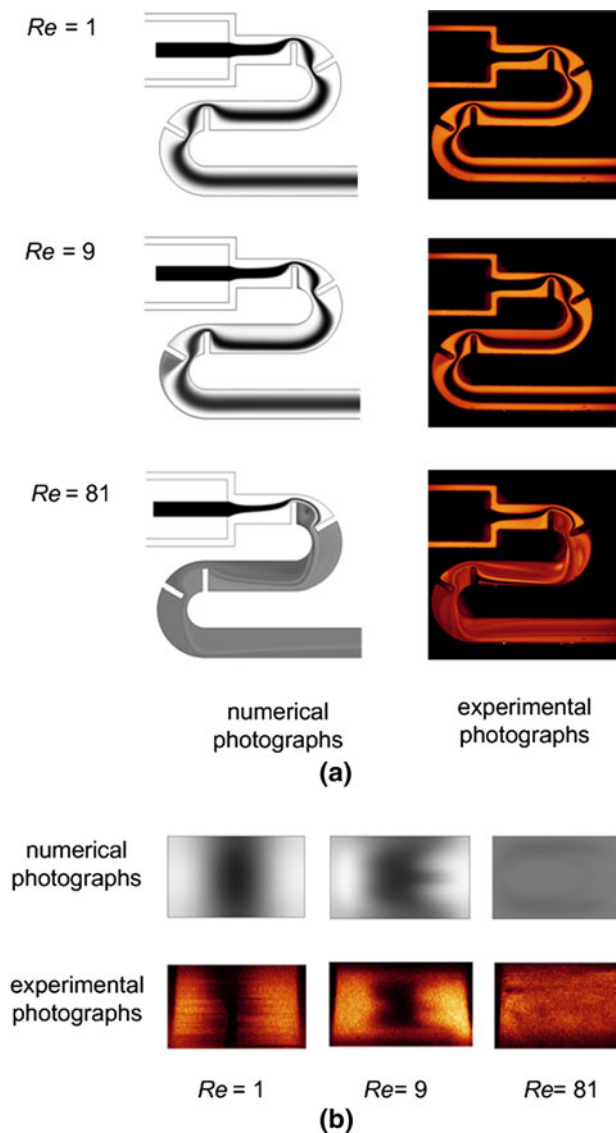
Fig. 2 Concentration distributions of the FTS CSC micromixer: **a** on the horizontal midplane, **b** at the exit for the cases with $Re = 1$, 9, and 81
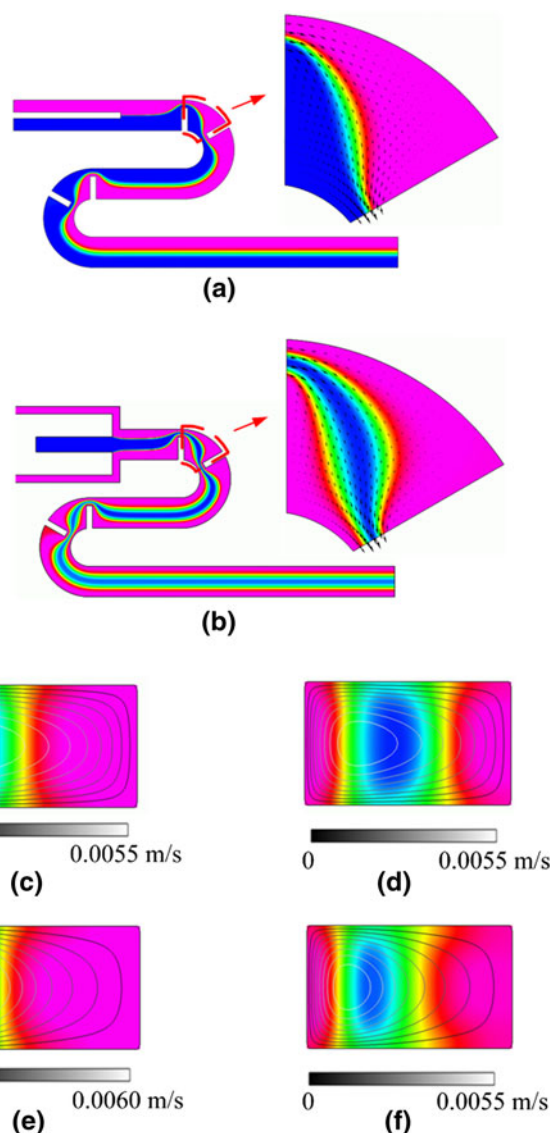

Fig. 3 Flow patterns and concentration distributions on the horizontal midplane: **a** the original CSC micromixer and **b** the FTS CSC micromixer; velocity contours and concentration distributions on the transverse cross sections of the first mixing unit: **c** on the $\theta = 30°$ plane of the original CSC micromixer, **d** on the $\theta = 30°$ plane of the FTS CSC micromixer, **e** on the $\theta = 90°$ plane of the original CSC micromixer, and **f** on the $\theta = 90°$ plane of the FTS CSC micromixer for the case with $Re = 0.3$

between the two fluids and the stream interfaces in the FTS CSC micromixer appear around the region with less streamwise velocity. Thus, the residence time of the stream interfaces between the two fluids in the FTS CSC micromixer is greater than that in the original CSC micromixer. Because of the above reasons, we may expect that the fluid mixing in the FTS CSC micromixer is significantly better than that in the original CSC micromixer for both small and large Reynolds numbers. Figure 4 shows that the expansion vortices after baffles and Dean vortices in the curved channel distort the interface between the two fluids and increase the interfacial area for the case with $Re = 27$. Thus, the fluid mixing in the flow with $Re = 27$ is better than that in the flow with $Re = 0.3$.

Next, we consider the three proposed CSC micromixers with three streams in the mixing units constructed by curved channels with baffles. Since the CSC micromixers enhance fluid mixing mainly by advection, the concentration distributions in the three micromixers for the cases with $Re = 81$ are shown in Figs. 5, 6, 7. We may find that the expansion vortices develop behind the radial baffles and the Dean vortices due to the continuous action of centrifugal force appear in the curved channel. These vortices stretch and deform the interfaces between the
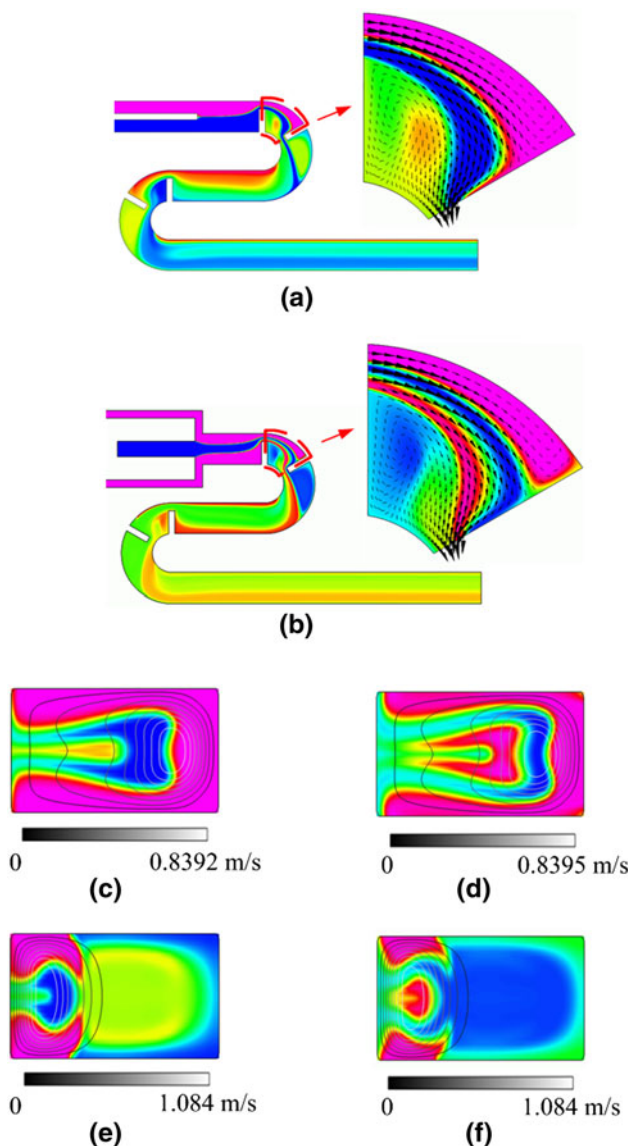
Fig. 4 Flow patterns and concentration distributions on the horizontal midplane: **a** the original CSC micromixer and **b** the FTS CSC micromixer; velocity contours and concentration distributions on the transverse cross sections of the first mixing unit: **c** on the $\theta = 30°$ plane of the original CSC micromixer, **d** on the $\theta = 30°$ plane of the FTS CSC micromixer, **e** on the $\theta = 90°$ plane of the original CSC micromixer, and **f** on the $\theta = 90°$ plane of the FTS CSC micromixer for the case with $Re = 27$
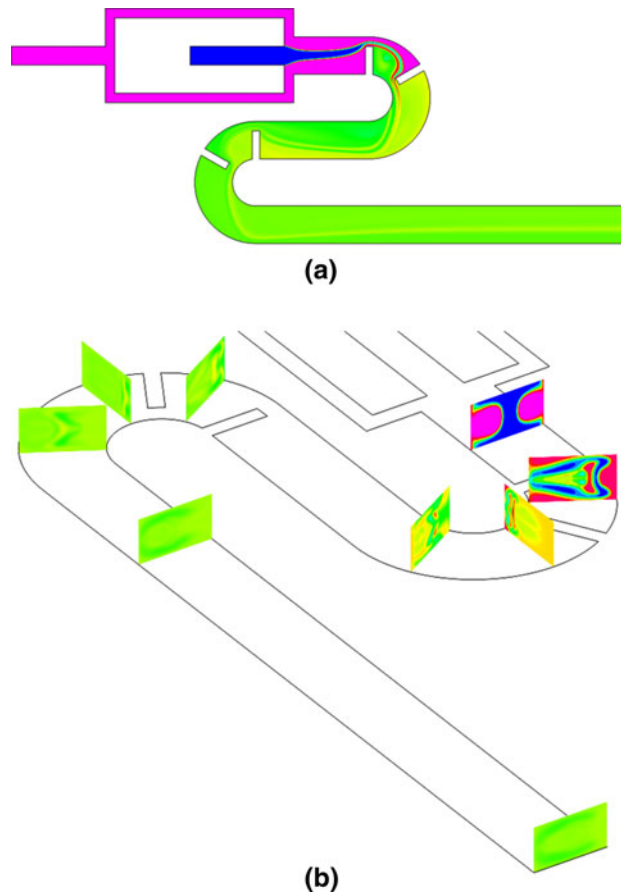

Fig. 5 **a** Concentration distribution on the horizontal midplane and **b** concentration distributions on the transverse cross sections of the FTS CSC micromixer for the case with $Re = 81$

mixing fluids, as shown in Figs. 5, 6, 7, and so enhance mixing efficiency. The FTS CSC micromixer generates the sandwiched structure of the streams at the starting point of the main channel. The flow velocity through the first passage of the FTS CSC micromixer is larger than that of the others, and so the expansion vortex behind the first baffle is the strongest among the three micromixers, as shown in Fig. 8. When the radius of the curved channel is small enough and the Reynolds number is large enough, an extra separation vortex develops in the down stream of the

second baffle attached to the external cylinder of the CSC channel (Tsai and Wu 2011). Comparing the extra separation vortex developing in the downstream of the second baffle of the three micromixers shown in Fig. 8, we find that the extra separation vortex of the FTS CSC micromixer is the largest and that of the CSC channel with ISI is the smallest. Therefore, the FTS CSC micromixer generates the largest interfacial area of mixing fluids and its performance is superior to that of other micromixers. Figure 6 shows that in the CSC microchannel with ISI the stream injected from the internal side-wall inlet pushes the expansion vortex behind the first baffle in the first mixing unit toward the external cylindrical wall, and the injected stream flows along the internal cylinder wall and is not involved in the vortex stirring behind the second baffle. Thus, the mixing efficiency of the CSC microchannel with ISI is inferior to that of others. Figure 7 shows that the stream injected from the external side-wall injection pushes the expansion vortex toward the internal cylinder wall and weakens the vortex stirring, and the thickness of the concentration lamella in the central region is thicker than that of the FTS CSC micromixer. Thus, the mixing efficiency of
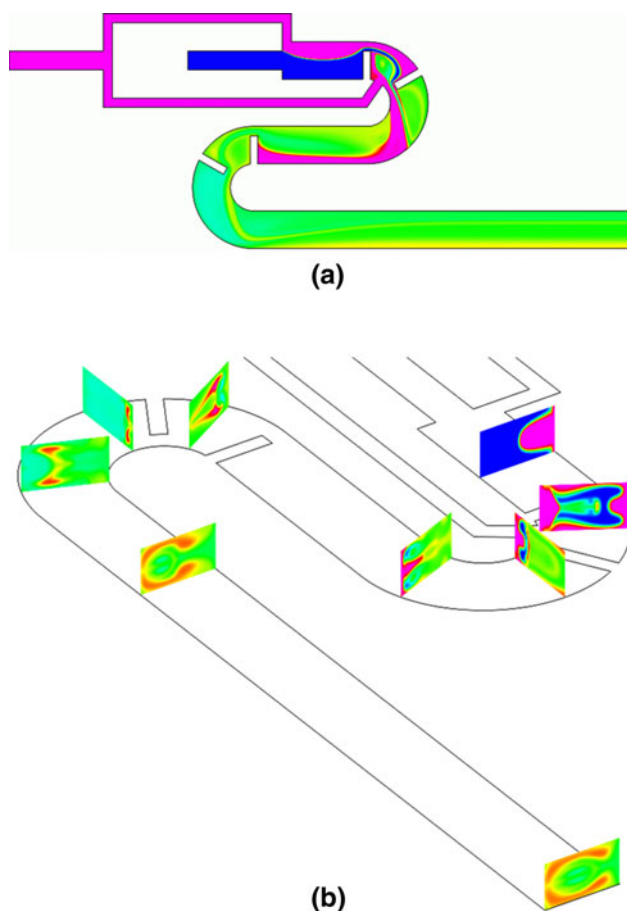
Fig. 6 **a** Concentration distribution on the horizontal midplane and **b** concentration distributions on the transverse cross sections of the CSC microchannel with ISI for the case with $Re = 81$
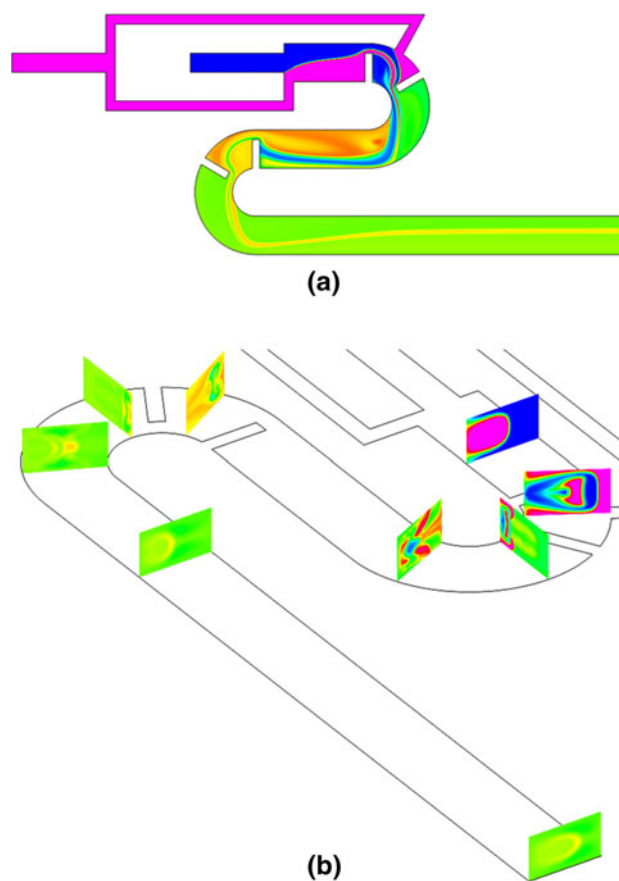

Fig. 7 **a** Concentration distribution on the horizontal midplane and **b** concentration distributions on the transverse cross sections of the CSC microchannel with ESI for the case with $Re = 81$

the CSC microchannel with ESI is less than that of the FTS CSC micromixer and greater than that of the CSC microchannel with ISI.

Figure 9 shows the degree of mixing at the exit cross section for the FTS CSC micromixer and other three types of micromixers over a wide range of Re. From Fig. 9, we may find the following trends. (i) The geometric sandwiched structure of streams increases the interfacial area between the two fluids to speed up mixing, especially for the full three-stream design. Hence, the fluid mixing in the FTS CSC micromixer is significantly better than that in the original CSC micromixer for all the Reynolds numbers considered. (ii) When the Reynolds number is large enough, the mixing is dominated by the expansion vortices and the lateral advection caused by the continuous action of centrifugal force. The degree of mixing of the original CSC micromixer may be greater than that of the CSC microchannel with ISI, due to the stream injected from the internal side-wall inlet is not involved in the expansion vortex behind the baffle in the first mixing chamber, as shown in Fig. 6. (iii) The performance of the four types of

micromixers depends on the Reynolds number strongly. The long residence time is beneficial to diffusion and leads to a good mixing efficiency for the cases with low Reynolds numbers. The residence time decreases and the effect of convection caused by the channel curvature or the radial baffles increases with the increase of the Reynolds number. When the Reynolds number is not very large ($Re \leq 3$), the effect of diffusion is stronger than that of convection, and so the mixing efficiency decreases with the increase of the Reynolds number first. However, when the Reynolds number is large enough, the effect of convection becomes dominant and the mixing efficiency increases with the increase of the Reynolds number. Thus, the valley of the mixing efficiency curve appears at a middle value of the Reynolds number, such as 3. Furthermore, for the case with a very small Reynolds number ($Re = 0.03$) the effect of side-wall injections is less important, and so the performance of the three-stream micromixers is almost equal, and is better than that of the original CSC micromixer.

Figure 10 shows the pressure applied increases with the increase of Reynolds number. The micromixers compared

Fig. 8 Flow patterns on the horizontal plane $z = 60$ μm and on the transverse cross section at $\theta = 90°$ for the case with $Re = 81$: **a**, **b** the FTS CSC micromixer, **c**, **d** the CSC microchannel with ISI, and **e** and **f** the CSC microchannel with ESI
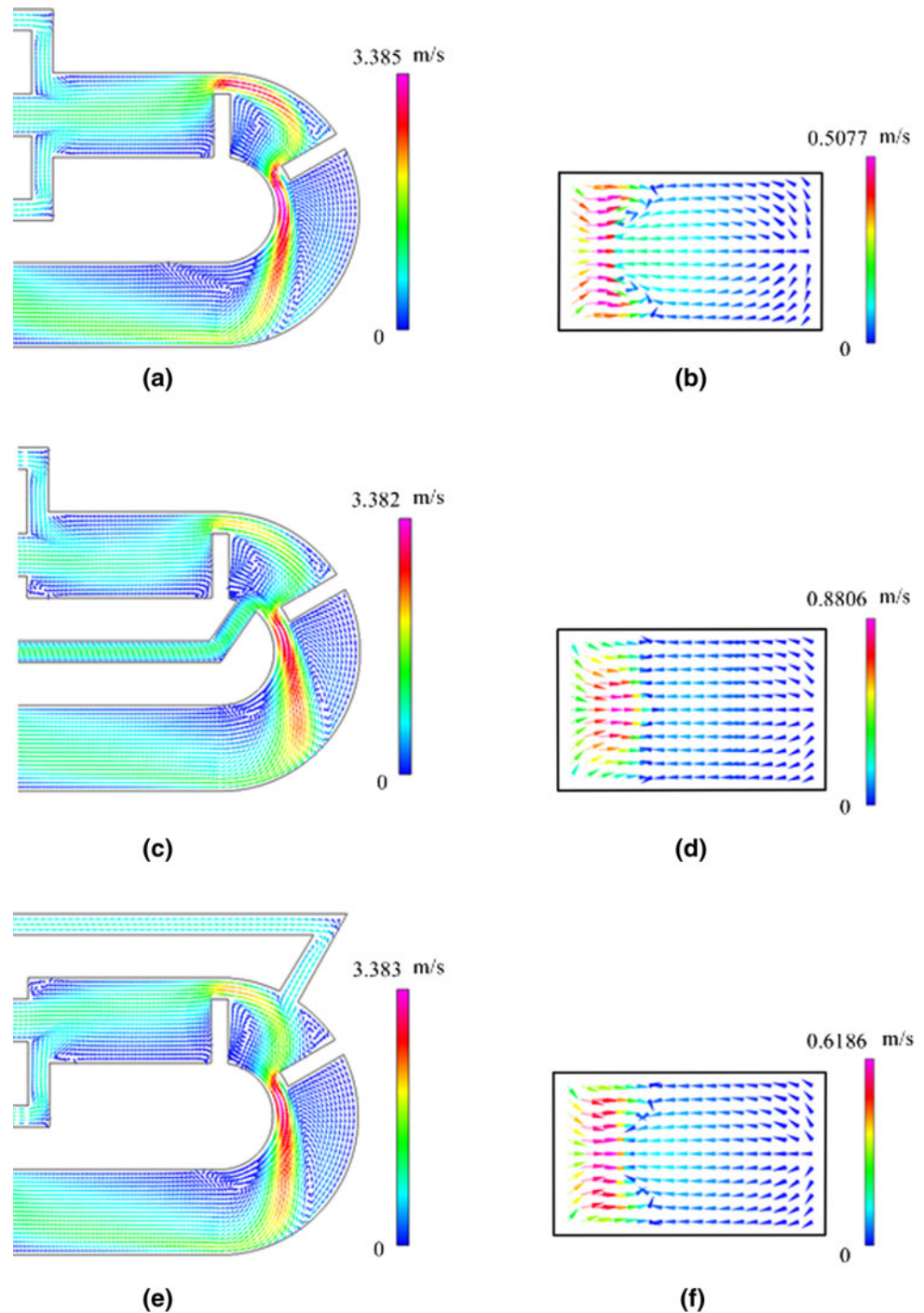
have the same length from the entrance to the exit along the central line of the channel ($L_p = L_e + 2\pi R_c + L_c + L_o$). The pressure applied to the flow is not sensitive to the location of side-wall injections. Thus, the pressure applied by these three types of three-stream micromixers is nearly the same, when they have the same side-wall injection width, passage width and number of baffles. However, the degree of mixing of the FTS CSC micromixer is greater than that of others. Therefore, the FTS CSC micromixer do

improve the performance of mixing with the same cost of pressure applied as other micromixers considered.

6 Conclusion

In this work, we design and fabricate three types of three-stream CSC micromixers, and compare those three-stream micromixers with the original CSC micromixer. We
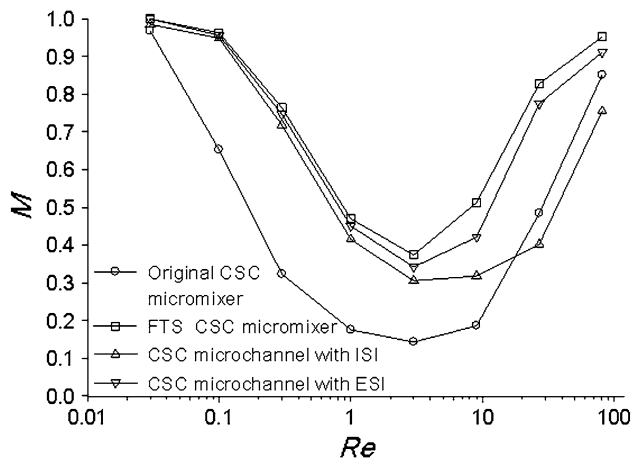
Fig. 9 Degrees of mixing at the exits of the FTS CSC micromixer, the CSC microchannel with ISI, the CSC microchannel with ESI and the original CSC micromixer for the cases with $Re = 0.03, 0.1, 0.3, 1, 3, 9, 27,$ and 81
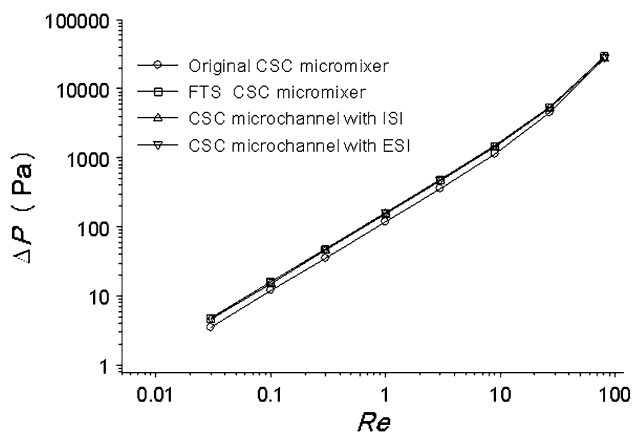

Fig. 10 Pressures applied between the entrance and the outlet of the FTS CSC micromixer, the CSC microchannel with ISI, the CSC microchannel with ESI and the original CSC micromixer for the cases with $Re = 0.03, 0.1, 0.3, 1, 3, 9, 27,$ and 81

examine fluid mixing in the proposed micromixers by numerical simulation and using confocal spectral microscope imaging system. The simulation results are in reasonable agreement with the experimental results. The sandwiched structure of streams, the multidirectional vortices, and the converging–diverging of flow through the passages contribute together to enhance mixing. Comparisons of the performance of the FTS CSC micromixer, the CSC microchannel with ISI and the CSC microchannel with ESI show that the FTS CSC micromixer is the preferable one among the three micromixers.

References

Abonnenc M, Josserand J, Girault HH (2009) Sandwich mixer-reactor: influence of the diffusion coefficient and flow rate ratios. Lab Chip 9:440–448

Bhagat AAS, Peterson ETK, Papautsky I (2007) A passive planar micromixer with obstructions for mixing at low Reynolds numbers. J Micromech Microeng 17:1017–1024

Boss J (1986) Evaluation of the homogeneity degree of a mixture. Bulk Solids Handl 6:1207–1215

Bothe D, Stemich C, Warnecke H-J (2006) Fluid mixing in a T-shaped micro-mixer. Chem Eng Sci 61:2950–2958

Chen H, Meiners J-C (2004) Topologic mixing on a microfluidic chip. Appl Phys Lett 84:2193–2195

Chung CK, Wu C-Y, Shih TR (2008) Effect of baffle height and Reynolds number on fluid mixing. Microsyst Technol 14:1317–1323

Hessel V, Hardt S, Löwe H, Schönfeld F (2003) Laminar mixing in different interdigital micromixer: I. Experimental characterization. AIChE J 49:566–577

Hessel V, Löwe H, Schönfeld F (2005) Micromixers—a review on passive and active mixing principles. Chem Eng Sci 60:2479–2501

Jiang F, Drese KS, Hardt S, Küpper M, Schönfeld F (2004) Helical flows and chaotic mixing in curved micro channels. AIChE J 50:2297–2305

Knight JB, Vishwanath A, Brody JP, Austin RH (1998) Hydrodynamic focusing on a silicon chip: mixing nanoliters in microseconds. Phy Rev Lett 80:3863–3866

Lee MG, Choi S, Park J-K (2010) Rapid multivortex mixing in an alternately formed contraction-expansion array microchannel. Biomed Microdevices 12:1019–1026

Liu RH, Stremler MA, Sharp KV, Olsen MG, Santiago JG, Adrian RJ, Aref H, Beebe DJ (2000) Passive mixing in a three-dimensional serpentine microchannel. J Microelectromech Syst 9:190–197

Nguyen N-T, Wu Z (2005) Micromixers—a review. J Micromech Microeng 15:R1–R16

Rani SA, Pitts B, Stewart PS (2005) Rapid diffusion of fluorescent tracers into *Staphylococcus epidermidis* biofilms visualized by time lapse microscopy. Antimicrob Agents Chemother 49:728–732

Stroock AD, Dertinger SKW, Ajdari A, Mezic I, Stone HA, Whitesides GM (2002) Chaotic mixer for microchannel. Science 295:647–651

Sudarsan AP, Ugaz VM (2006) Multivortex micromixing. Proc Natl Acad Sci USA 103:7228–7233

Tay FEH (2002) Microfluidics and BioMEMS applications. Kluwer Academic, Boston, pp 155–163

Tsai R-T, Wu C-Y (2011) An efficient micromixer based on multidirectional vortices due to baffles and channel curvature. Biomicrofluidics 5:014103

Wang H, Iovenitti P, Harvey E, Masood S (2002) Optimizing layout of obstacles for enhanced mixing in microchannels. Smart Mater Struct 11:662–667

Wu Z, Nguyen N-T (2005) Convective-diffusive transport in parallel lamination micromixers. Microfluid Nanofluid 1:208–217

Yi M, Bau HH (2003) The kinematics of bend-induced mixing in micro-conduits. Int J Heat Fluid Flow 24:645–656